

# Gang Mu

## List of Publications by Year in descending order

Source: <https://exaly.com/author-pdf/323612/publications.pdf>

Version: 2024-02-01

118  
papers

3,926  
citations

172457  
29  
h-index

123424  
61  
g-index

124  
all docs

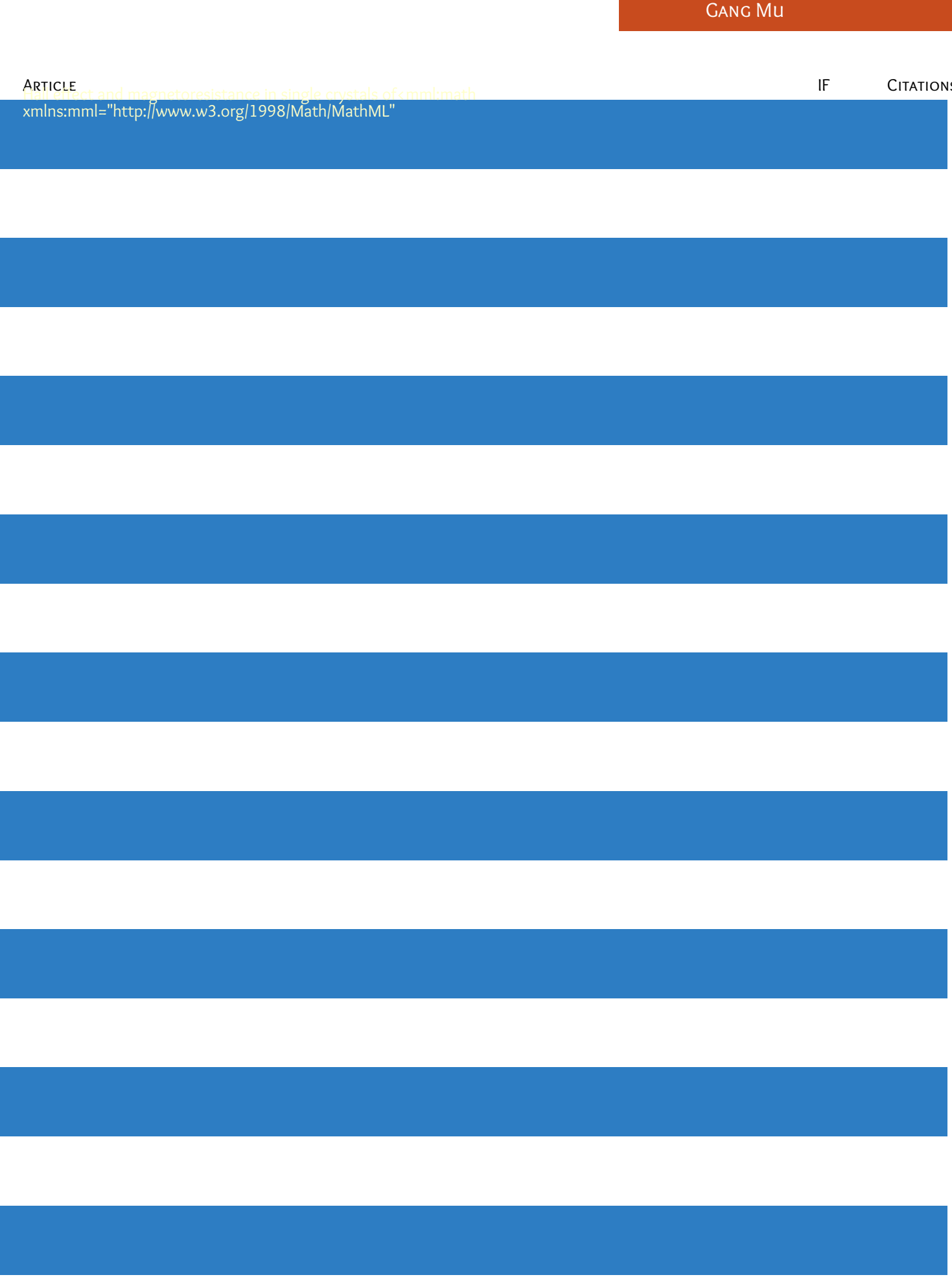
124  
docs citations

124  
times ranked

3674  
citing authors

#	ARTICLE	IF	CITATIONS
1	Superconductivity at 25 K in hole-doped (La <sub>1-x</sub> Sr <sub>x</sub> )OFeAs. <i>Europhysics Letters</i> , 2008, 82, 17009.	2.0	538
2	Transition of stoichiometric $\text{Sr}_{2-x}\text{Fe}_2\text{As}_2$ to a superconducting state at 37.2 K. <i>Physical Review B</i> , 2009, 79, .		
3	Roles of multiband effects and electron-hole asymmetry in the superconductivity and normal-state properties of $\text{Sr}_{2-x}\text{Fe}_2\text{As}_2$ . <i>Physical Review B</i> , 2009, 79, .		

#	ARTICLE	IF	CITATIONS
19	The effect and magnetoresistance in single crystals of $\text{cmn}(\text{math}\text{ml})$ xmlns:mml="http://www.w3.org/1998/Math/MathML"		



#	ARTICLE	IF	CITATIONS
37	Growth and characterization of millimeter-sized single crystals of CaFeAsF. <i>Superconductor Science and Technology</i> , 2015, 28, 085008.	3.5	21
38	Low temperature specific heat of 12442-type KCa <sub>2</sub> Fe <sub>4</sub> As <sub>4</sub> F <sub>2</sub> single crystals. <i>Science China: Physics, Mechanics and Astronomy</i> , 2020, 63, 1.	5.1	21
39	Quantum spin correlations through the superconducting-to-normal phase transition in electron-doped superconducting Pr <sub>0.88</sub> LaCe <sub>0.12</sub> CuO <sub>4-δ</sub> . <i>Proceedings of the National Academy of Sciences of the United States of America</i> , 2007, 104, 15259-15263.	7.1	19
40	Doping Dependence of Superconductivity and Lattice Constants in Hole Doped La <sub>1-x</sub> Sr <sub>x</sub> FeAsO. <i>Journal of the Physical Society of Japan</i> , 2008, 77, 15-18.	1.6	19
41	Structural and transport properties of Sr <sub>2</sub> VO <sub>3</sub> -FeAs superconductors with different oxygen deficiencies. <i>Science China: Physics, Mechanics and Astronomy</i> , 2010, 53, 1202-1206.	5.1	19
42	Specific heat and phase diagrams of single crystal iron pnictide superconductors. <i>Physica C: Superconductivity and Its Applications</i> , 2009, 469, 575-581.	1.2	18
43	Possible two-gap behavior in noncentrosymmetric superconductor $\text{Mg}_{3-\frac{2}{x}}\text{Fe}_{10}$ . A penetration depth study. <i>Physical Review B</i> , 2009, 79, .		
44	Evidence for line nodes in the energy gap of the overdoped Ba(Fe <sub>1-x</sub> Cox) <sub>2</sub> As <sub>2</sub> from low-temperature specific heat measurements. <i>Physical Review B</i> , 2011, 84, .	3.2	18
45	Fermi Surface with Dirac Fermions in CaFeAsF Determined via Quantum Oscillation Measurements. <i>Physical Review X</i> , 2018, 8, .	8.9	18
46	Iron-doped VSe <sub>2</sub> nanosheets for enhanced hydrogen evolution reaction. <i>Applied Physics Letters</i> , 2020, 116, .	3.3	18
47	Growth and characterization of single crystals. <i>Journal of Crystal Growth</i> , 2007, 305, 222-227.	1.5	17
48	Parent phase and superconductors in the fluorine derivative family. <i>Physica C: Superconductivity and Its Applications</i> , 2009, 469, 381-384.	1.2	17
49	Effect of Local Structure Distortion on Superconductivity in Mg- and F-Codoped LaOBiS <sub>2</sub> . <i>Inorganic Chemistry</i> , 2014, 53, 9-11.	4.0	17
50	Growth and characterization of CaFe <sub>1</sub> -Co AsF single crystals by CaAs flux method. <i>Journal of Crystal Growth</i> , 2016, 451, 161-164.	1.5	17
51	Anisotropic physical properties and large critical current density in $\text{Ca}_{0.882}\text{Fe}_{0.118}\text{AsF}_3$ . <i>Physical Review Materials</i> , 2020, 4, .		
52	Ferromagnetic CoSe broadband photodetector at room temperature. <i>Nanotechnology</i> , 2020, 31, 374002.	2.6	15
53	Strong anisotropy effect in an iron-based superconductor CaFe <sub>0.882</sub> Co <sub>0.118</sub> AsF. <i>Superconductor Science and Technology</i> , 2017, 30, 074003.	3.5	14
54	Elastoresistance measurements on $\text{Ca}_{0.882}\text{Fe}_{0.118}\text{AsF}_3$ and $\text{KCa}_{0.882}\text{Fe}_{0.118}\text{AsF}_3$ . <i>Physical Review B</i> , 2020, 102, .	3.2	14

#	ARTICLE	IF	CITATIONS
55	Universal linear-temperature resistivity: possible quantum diffusion transport in strongly correlated superconductors. <i>Scientific Reports</i> , 2017, 7, 9469.	3.3	13
56	Strong In-Plane Magnetic Field-Induced Reemergent Superconductivity in the van der Waals Heterointerface of $\text{NbSe}_{2}$ and $\text{CrCl}_3$ . <i>ACS Applied Materials &amp; Interfaces</i> , 2020, 12, 49252-49257.	8.0	13
57	Electron and Hole Injection via Charge Transfer at the Topological Insulator $\text{Bi}_{2\bar{x}}\text{Sb}_{x}\text{Te}_{3-y}\text{Se}_{y}$ Organic Molecule Interface. <i>Journal of Physical Chemistry C</i> , 2014, 118, 3533-3538.	3.1	12
58	Power-law-like correlation between condensation energy and superconducting transition temperatures in iron pnictide/chalcogenide superconductors: Beyond the BCS understanding. <i>Physical Review B</i> , 2014, 89, .	3.2	12
59	Effects of electron correlation, electron-phonon coupling, and spin-orbit coupling on the isostructural $\text{Pd}$ -substituted superconductor $\text{SrPt}_3$ . <i>Physical Review B</i> , 2016, 93, .	1.2	11
60	Suppression of backward scattering of Dirac fermions in iron pnictides $\text{Ba}(\text{Fe}_{1-x}\text{Ru}_x\text{As})_2$ . <i>Physical Review B</i> , 2012, 86, .	3.2	11
61	Unusual evolution of $B_{\text{c}2}$ and $T_{\text{c}}$ with inclined fields in restacked $\text{TaS}_2$ nanosheets. <i>Npj Quantum Materials</i> , 2018, 3, .	5.2	11
62	Absence of Superconductivity in $\text{LiCu}_2\text{P}_2$ . <i>Journal of the American Chemical Society</i> , 2011, 133, 1751-1753.	13.7	10
63	Low-Temperature Physical Properties of $\text{Ba}_8\text{Ni}_x\text{Ge}_{46-x}$ ( $x=3, 4, 6$ ). <i>Journal of Electronic Materials</i> , 2012, 41, 1177-1180.	2.2	10
64	Pressure-induced superconductivity in parent $\text{CaFeAsF}$ single crystals. <i>Physical Review B</i> , 2018, 97, .	3.2	10
65	A structural study of the hole-doped superconductors $\text{Pr}_{1-x}\text{Sr}_x\text{FeAsO}$ . <i>New Journal of Physics</i> , 2009, 11, 083003.	2.9	9
66	Specific heat of optimally doped $\text{Ba}(\text{Fe}_{1-x}\text{Mn}_x\text{As})_2$ . <i>Europhysics Letters</i> , 2010, 91, 10001.	3.2	9
67	$\lambda$ - $\text{FeAs}$ : Magnetic-field-induced metal-insulator quantum phase transition in $\text{CaFeAsF}$ near the quantum limit. <i>Science China: Physics, Mechanics and Astronomy</i> , 2018, 61, 1.	5.1	9
68	Superconductivity at 15.6%K in calcium-doped $\text{Tb}_{1-x}\text{Ca}_x\text{FeAsO}$ : The structure requirement for achieving superconductivity in the hole-doped 1111 phase. <i>Europhysics Letters</i> , 2010, 89, 27002.	2.0	8
69	Heat capacity studies on rattling vibrations in $\text{Ba}_{1-x}\text{TM}_x\text{Ge}$ type I clathrates. <i>Journal of Physics and Chemistry of Solids</i> , 2012, 73, 1521-1523.	4.0	8
70	Synthesis, Structural, and Transport Properties of Cr-Doped $\text{BaTi}_2\text{As}_2\text{O}$ . <i>Inorganic Chemistry</i> , 2014, 53, 13089-13092.	4.0	8
71	Synthesis and structures of type-I clathrates: $\text{Rb}_6\text{Na}_2\text{Ge}_{44.89(1)}$ , $\text{Cs}_6\text{Na}_2\text{Zn}_4\text{Ge}_{42}$ and $\text{Cs}_6.40(1)\text{Na}_1.60(1)\text{Ga}_8\text{Ge}_{38}$ . <i>Journal of Solid State Chemistry</i> , 2016, 242, 155-161.	2.9	8
72	Superconductivity in Ti-doped iron-arsenide compound $\text{Sr}_4\text{Cr}_0.8\text{Ti}_{1.2}\text{O}_6\text{Fe}_2\text{As}_2$ . <i>Science in China Series G: Physics, Mechanics and Astronomy</i> , 2009, 52, 1876-1878.	0.2	7

#	ARTICLE	IF	CITATIONS
73	Observation of two-dimensional superconductivity in an ultrathin iron-arsenic superconductor. <i>2D Materials</i> , 2021, 8, 025024.	4.4	7
74	Structure and properties of type-II clathrate Cs <sub>8</sub> Na <sub>16</sub> Tl <sub>x</sub> Ge <sub>136</sub> . <i>Dalton Transactions</i> , 2015, 44, 16937-16945.	3.3	6
75	Two-gap superconductivity in CaFe <sub>0.88</sub> Co <sub>0.12</sub> AsF revealed by temperature dependence of the lower critical field H <sub>c1c</sub> (T). <i>Npj Quantum Materials</i> , 2019, 4, .	5.2	6
76	Superconductivity in the hole-doped oxy-arsenide RE <sub>1-x</sub> SrxFeAsO (RE=La, Pr). <i>Physica C: Superconductivity and Its Applications</i> , 2009, 469, 894-897.	1.2	5
77	Enhancement of superconductivity by Sb-doping in the hole-doped iron-pnictide superconductor Pr <sub>1-x</sub> SrxFeAsO. <i>Physica C: Superconductivity and Its Applications</i> , 2014, 498, 50-53.	1.2	5
78	Type-I clathrates of K <sub>7.69(2)</sub> Cu <sub>2.94(6)</sub> Ge <sub>43.06(6)</sub> and Rb <sub>8</sub> Ag <sub>2.79(4)</sub> Ge <sub>43.21(4)</sub> . <i>RSC Advances</i> , 2015, 5, 53829-53834.	3.6	5
79	Synthesis, Crystal Structure, and Physical Properties of Layered <i>i</i> Ln <sub>2</sub> CrSe <sub>2</sub> ( <i>i</i> Ln = Ce-Nd). <i>Inorganic Chemistry</i> , 2019, 58, 9482-9489.	4.0	5
80	The transport properties in graphene/single-unit-cell cuprates van der Waals heterostructure. <i>Superconductor Science and Technology</i> , 2019, 32, 085007.	3.5	5
81	Gap Structure of 12442-Type KCa <sub>2</sub> (Fe <sub>1-x</sub> Co <sub>x</sub> ) T <sub>j</sub> ETQq1 1 0.784314 rgBT /Overlock 10 Tf 50 427 Td Lower Critical Field. <i>Chinese Physics Letters</i> , 2020, 37, 127401.	3.3	5
82	Low temperature specific heat in BaFe <sub>1.9</sub> Ni <sub>0.1</sub> As <sub>2</sub> single crystals. <i>Science China: Physics, Mechanics and Astronomy</i> , 2010, 53, 1221-1224.	5.1	4
83	Impurity scattering effect in Pd-doped superconductor SrPt <sub>3</sub> P. <i>Frontiers of Physics</i> , 2016, 11, 1.	5.0	4
84	In situ annealing effects on magnetic properties and variable-range hopping of iron-based ladder material BaFe <sub>2</sub> S <sub>3</sub> . <i>Science China: Physics, Mechanics and Astronomy</i> , 2018, 61, 1.	5.1	4
85	Charge-Transfer-Induced Intermittent Exchange Coupling at the $\text{Co}_{\text{Fe}}/\text{Fe}$ Interface. <i>Physical Review Applied</i> , 2019, 12,	3.8	4
86	Gate-tunable two-dimensional superconductivity revealed in flexible wafer-scale hybrid structures. <i>Journal of Materials Chemistry C</i> , 2020, 8, 14605-14610.	5.5	4
87	Phase evolution with the film thickness in PLD-grown titanium oxides films. <i>Journal of Alloys and Compounds</i> , 2020, 831, 154727.	5.5	4
88	Multiband effect in the noncentrosymmetric superconductors $\text{Mg}_{3/2}\text{Mn}_{12}$ by H. <i>Physical Review B</i> , 2010, 82,	3.2	4
89	Selenium doping in potential topological superconductor Sn <sub>0.8</sub> In <sub>0.2</sub> Te. <i>Journal of Solid State Chemistry</i> , 2015, 229, 124-128.	2.9	3
90	Synthesis, Structure, and Properties of Clathrate Si <sub>30.3(8)</sub> P <sub>15.7(8)</sub> Se <sub>7.930(3)</sub> . <i>Chemistry - A European Journal</i> , 2017, 23, 9505-9516.	3.3	3

#	ARTICLE	IF	CITATIONS
91	Optimization of synthesis parameters and pressure effect for layered honeycomb ruthenate SrRu2O6. Journal of Alloys and Compounds, 2020, 816, 152672.	5.5	3
92	Evidence for ferromagnetic order in the CoSb layer of LaCoSb2. Physical Review B, 2020, 101, .	3.2	3
93	Anisotropic thermally activated flux-flow behavior in the layered superconductor $\text{R}_{\text{h}1-\text{x}}\text{Co}_{\text{x}}\text{As}_2$ . Physical Review B, 2021, 103, .	3.2	3
94	One-step synthesis of nitrogen-rich $\text{Mo}_2\text{C}_{1-x}\text{Nx}$ solid solution with enhanced superconductivity. Journal of Materials Chemistry C, 2020, 8, 2682-2686.	5.5	3
95	Observation of above-room-temperature ferromagnetism in chemically stable layered semiconductor $\text{R}_{\text{h}1-\text{x}}\text{Co}_{\text{x}}\text{As}_2$ . 2D Materials, 2020, 7, 045034.	4.4	3
96	Topological frequency shift of quantum oscillation in CaFeAsF. Npj Quantum Materials, 2022, 7, .	5.2	3
97	Physical properties of the new superconducting system $\text{Sr}_2\text{VO}_3\text{FeAs}$ (21311). Physica C: Superconductivity and Its Applications, 2010, 470, S263-S266.	1.2	2
98	Superconductivity induced by U doping in the SmFeAsO system. Physical Review B, 2013, 87, .	3.2	2
99	New clathrates of $\text{Rb}_{7.50(1)}\text{Tl}_{0.50(1)}\text{Ge}_{46}$ and $\text{K}_{7.62(1)}\text{Tl}_{0.38(1)}\text{Ge}_{45.34(3)}$ . RSC Advances, 2016, 6, 75269-75276.	3.6	2
100	Multiple gaps revealed by low temperature specific heat in the 1111-type $\text{CaFe}_{0.88}\text{Co}_{0.12}\text{AsF}$ single crystals. Journal of Physics Condensed Matter, 2019, 31, 455602.	1.8	2
101	Upper critical field and its anisotropy in $\text{RbCr}_{3}\text{As}_3$ . Physical Review B, 2019, 100, .	3.2	2
102	Chemical vapor deposition growth and characterization of graphite-like film. Materials Research Express, 2020, 7, 015609.	1.6	2
103	Critical Current Density and Vortex Dynamics in Pristine and Irradiated $\text{KC}_{2}\text{Fe}_4\text{As}_4\text{F}_2$ . Materials, 2021, 14, 5283.	2.9	2
104	Investigation of the flux dynamics in $\text{KC}_{2}\text{Fe}_4\text{As}_4\text{F}_2$ single crystal by ac susceptibility measurements. Superconductor Science and Technology, 2022, 35, 055013.	3.5	2
105	Pressure effect in the antiperovskite phosphide superconductor $\text{Sr}_{2}\text{Fe}_2\text{As}_4\text{F}_2$ . Physical Review B, 2022, 105, .	3.2	2
106	Low-Temperature Physical and Thermoelectric Properties of $\text{Ba}_8\text{Ni}_5\text{Ge}_4$ . Journal of Electronic Materials, 2013, 42, 2025-2029.	2.2	1
107	A Field-Directional Specific Heat Study on the Gap Structure of Overdoped $\text{Ba}(\text{Fe}_{1-\text{x}}\text{Co}_{\text{x}})_2\text{As}_2$ . Journal of the Physical Society of Japan, 2013, 82, 054714.	1.6	1
108	Phase diagram and weak-link behavior in Nd-doped CaFe <sub>2</sub> As <sub>2</sub> . New Journal of Physics, 2014, 16, 113024.	2.9	1

#	ARTICLE	IF	CITATIONS
109	Germanium isotope effect induced guest rattling and cage distortion in clathrates. <i>Journal of Materomics</i> , 2018, 4, 338-344.	5.7	1
110	Anomalous high-field magnetotransport in CaFeAsF due to the quantum Hall effect. <i>Npj Quantum Materials</i> , 2022, 7, .	5.2	1
111	Anisotropic superconducting order parameters in the iron pnictide superconductors. <i>Journal of Physics: Conference Series</i> , 2012, 400, 022135.	0.4	0
112	Quantum magnetoresistance in the Ca-intercalated graphite superconductor CaC <sub>6</sub> . <i>Physical Review B</i> , 2014, 90, .	3.2	0
113	Electronic and magnetic structures of the ferroelectric compound $\text{PbBaFe}_{3.2}O_5$ . <i>Physical Review B</i> , 2015, 91, .	3.2	0
114	Gap Structure of the Overdoped Iron-Pnictide Superconductor Ba(Fe <sub>0.942</sub> Ni <sub>0.058</sub> ) <sub>2</sub> As <sub>2</sub> : A Low-Temperature Specific-Heat Study. <i>Advances in Condensed Matter Physics</i> , 2015, 2015, 1-5.	1.1	0
115	Exotic Superconductivity in Correlated Electron Systems. <i>Advances in Condensed Matter Physics</i> , 2015, 2015, 1-2.	1.1	0
116	Frontispiece: Synthesis, Structure, and Properties of Clathrate Si <sub>30.3</sub> (8)P <sub>15.7</sub> (8)Se <sub>7.930</sub> (3). <i>Chemistry - A European Journal</i> , 2017, 23, .	3.3	0
117	Hydrothermal synthesis, structure and magnetic properties of Ru doped La <sub>0.5</sub> Sr <sub>0.5</sub> MnO <sub>3</sub> . <i>Frontiers of Physics</i> , 2019, 14, 1.	5.0	0
118	Evolution of the upper critical field and superconducting vortex phase with thickness in PLD-grown Ta films. <i>Superconductor Science and Technology</i> , 2022, 35, 055010.	3.5	0